

Functional and Genetic Analysis of Viral Receptor ACE2 Orthologs Reveals Broad Potential Host Range of SARS-CoV-2

Yinghui Liu^{1*}, Gaowei Hu^{2*}, Yuyan Wang^{2*}, Xiaomin Zhao^{1*}, Fansen Ji¹, Wenlin Ren¹, Mingli Gong¹, Xiaohui Ju¹, Changhe Li¹, Junxian Hong¹, Yuanfei Zhu², Xia Cai², Jianping Wu^{3,4}, Xun Lan¹, Youhua Xie², Xinquan Wang^{5,6}, Zhenghong Yuan^{2†}, Rong Zhang^{2†}, Qiang Ding^{1,6†}

¹Center for Infectious Disease Research, School of Medicine, Tsinghua University, Beijing 100086, China.

²Key Laboratory of Medical Molecular Virology (MOE/NHC/CAMS), School of Basic Medical Sciences, Shanghai Medical College, Biosafety Level 3 Laboratory, Fudan University, Shanghai 200032, China.

³Key Laboratory of Structural Biology of Zhejiang Province, School of Life Sciences, Westlake University, 18 Shilongshan Road, Hangzhou 310024, Zhejiang Province, China.

⁴Institute of Biology, Westlake Institute for Advanced Study, 18 Shilongshan Road, Hangzhou 310024, Zhejiang Province, China.

⁵School of Life Sciences, Tsinghua University, Beijing 100086, China.

⁶Beijing Advanced Innovation Center for Structural Biology, Tsinghua University, Beijing 100086, China

†Corresponding authors: qding@tsinghua.edu.cn(Q.D.); rong_zhang@fudan.edu.cn (R.Z.); zhyuan@shmu.edu.cn (Z.Y.);

*These authors contributed equally to this work.

Abstract

The pandemic of a newly emerging coronavirus (SARS-CoV-2), the causative agent of severe pneumonia disease (COVID-19), is threatening global health. Epidemiological studies suggested that bats are the natural reservoir hosts for SARS-CoV-2, however, the host range of SARS-CoV-2 and the identity of intermediate hosts facilitating the transmission to humans remains unknown. Coronavirus–receptor interaction is a key genetic determinant of the host range, cross-species transmission, and tissue tropism. SARS-CoV-2 uses ACE2 as the receptor to enter the cells in a species-dependent manner, and it has been shown that human, palm civet, pig and bat ACE2 can support virus entry, but mouse ACE2 cannot. In this study, we aimed to characterize ACE2 from a diversity of species for its ability to support viral entry. We found that ACE2 is expressed in a wide range of host species, with high conservation especially in mammals. By analyzing critical amino acid residues in ACE2 for virus entry, based on the well-characterized SARS-CoV spike protein interaction with ACE2 (human, bat, palm civet, pig and ferret ACE2), we found approximately eighty ACE2 proteins from mammals could potentially function as the receptor to mediate SARS-CoV-2 entry. Functional assays showed that 44 of these mammalian ACE2 orthologs, including domestic animals, pet animals, livestock animals and even animals in the zoo or aquaria, could bind viral spike protein and support SARS-CoV-2 entry. In summary, our study demonstrated that ACE2 from a diversity of animal species could be utilized by SARS-CoV-2 to mediate viral entry, indicating it has a broad host range and highlighted that SARS-CoV-2 might be distributed much more widely than previously recognized, emphasizing the necessity to monitor the susceptible hosts, especially their potential of cross-species, which could prevent the future outbreaks.

Key words: COVID-19, SARS-CoV-2, ACE2, Host range, Intermediate host

Introduction

Coronaviruses are a group of positive-stranded, enveloped RNA viruses that circulate broadly among humans, other mammals, and birds, causing respiratory, enteric, or hepatic diseases (Perlman and Netland, 2009). In the last two decades, coronaviruses have caused two major outbreaks: SARS (Severe acute respiratory syndrome) and MERS (Middle East respiratory syndrome) (Graham et al., 2013). The recent outbreak of a novel severe pneumonia disease (COVID-19) has already caused 2,580,000 infection, leading to 178,000 death. The causative pathogen of COVID-19 is a novel coronavirus, SARS-CoV-2 (Wu et al., 2020; Zhou et al., 2020). Phylogenetic analyses suggest that SARS-CoV, MERS-CoV and SARS-CoV-2 likely originate from bats, with SARS-CoV spreading from bats to palm civets to humans, and MERS-CoV spreading from bats to camel to humans (Cui et al., 2019), however, the intermediate host of SARS-CoV-2 fueling spillover to humans remains unknown.

The SARS-CoV-2 encodes a spike protein, which binds with the cellular receptor angiotensin-converting enzyme II (ACE2) to mediate viral entry (Hoffmann et al., 2020; Zhou et al., 2020). It has been well characterized that the receptor-binding domain (RBD) of the spike protein is responsible for the interaction with ACE2. After the binding with ACE2, the spike protein was subsequently cleaved by the host protease to release the spike fusion peptide, which promote virus entry into the target cells (Hoffmann et al., 2020; Wan et al., 2020). It has been found that the interaction of virus with species-specific receptor is a primary determinant of host tropism and therefore constitutes a major interspecies barrier at the viral entry level (Douam et al., 2015). Previous studies found that murine ACE2 cannot efficiently bind with SARS-S protein to mediate viral entry into mouse cells, therefore, human ACE2 transgenic mouse was developed as an *in vivo* model to study the infection and pathogenesis of SARS-CoV and SARS-CoV-2 (Bao et al., 2020; Yang et al., 2007).

ACE2 is expressed in a diverse range of species through the *Vertebrata*. Several recent studies demonstrated that ferrets, cats, dogs and some non-human primates are susceptible to SARS-CoV-2 (Kim et al., 2020; Lu et al., 2020; Rockx et al., 2020; Shi et al., 2020; Zhang et al., 2020a). However, the exact host range of SARS-CoV-2 remains unknown and urgently needs to be explored. In this study, we characterized ACE2 from a diversity of species for its ability to support SARS-CoV-2 entry. Our data demonstrated that ACE2 from a diversity of animal species could be utilized by SARS-CoV-2 to mediate viral entry, suggesting that SARS-CoV-2 has a broad host range at the level of virus entry, which may facilitate its cross-species transmission and evolution.

RESULTS

Evolutionary and phylogenetic analysis of ACE2 orthologs from a diversity of species

ACE2, the cellular receptor for SARS-CoV-2 and SARS-CoV, is expressed in a diverse range of species through the *Vertebrata*. We analyzed 294 ACE2 orthologs in the NCBI database, including birds (75 species), alligators (4 species), turtles (4 species), lizards (9 species), mammals (129 species), amphibians (4 species), coelacanths (1 species), bone fishes (67 species) and cartilaginous fishes (1 species) (Fig. S1). These ACE2 orthologs range from 344 to 861 amino acid residues in length and are characterized by an N-terminal LRR domain and a C-terminal LCAR region. A series of structures of SARS-CoV spike protein complexed with human or other ACE2 orthologs have been solved, and 5 critical amino acid residues of ACE2 that are highly conserved and indispensable for interaction with viral spike protein and virus entry have been identified (Li, 2008, 2015; Li et al., 2005; Wan et al., 2020). Based on this structural information and conservation of those 5 critical amino acids, we carried out primary sequence alignment across the 294 ACE2 proteins (Fig. S1). Our analysis selected ACE2 orthologs from 80 species that could potentially function as the receptors of SARS-CoV-2 (Fig. S1, and Fig 1). All the 80 ACE2 orthologs are derived from mammals, including wild animals, domestic animals, pet animals, livestock animals and even animals in the zoo or aquaria, with protein size ranging from 790 to 811 amino acids (Table S1). Other ACE2 orthologs from mammals (49/129 species) that are predicted as non-functional receptors of SARS-CoV and SARS-CoV-2, including mouse and rat, are summarized and not included in this present study (Table S2).

We performed phylogenetic analysis of these 80 ACE2 orthologs with potential function to mediate virus infection, plus mouse and rat ACE2 proteins to elucidate the evolutionary of ACE2 proteins. Additionally, we aligned the twenty residues of ACE2 known to be located at the interface with ACE2 (Lan et al., 2020; Shang et al., 2020; Yan et al., 2020) (Fig 1). It showed that ACE2 protein sequences are highly conserved across the species analyzed here. Of note, the twenty residues at the interface of ACE2-spike complex are identical across the Catarrhini, including great apes and Old World monkeys. However, those residues in ACE2 from New World monkeys are less conserved, for example, Y41 and Q42 in human ACE2 responsible for the formation of hydrogen bonds with viral spike protein, highly conserved across all other species, are substituted by H and E in New World monkeys, respectively. In non-primate mammals, increasing number of substitutions are evident, even in the residues that can form hydrogen bonds or salt-bridges with spike protein, such as Q24, D30, D38, and Y83 (Fig. 1).

Collectively, our analysis suggested that ACE2 orthologs are highly conserved across a wide range of mammals, and a diversity of ACE2 orthologs in mammals might function as entry receptor for SARS-CoV-2.

Interaction of ACE2 proteins with SARS-CoV-2 spike protein

Based on the evolutionary analysis, we chose 48 representative ACE2 orthologs (Table S1 and Fig. 1), from *Primates*, *Rodentia*, *Cetartiodactyla*, *Chiroptera*, *Diprotodontia*, *Perissodactyla*, *Carnivora* and *Pholidota*, to assess their abilities to support SARS-CoV-2 entry by ectopic expression of each ACE2 ortholog in HeLa cells which have limited endogenous ACE2 expression (Zhou et al., 2020). These 48 species include wild animals, animals in the zoo and aquarium, pet animals and livestock in close contact with humans, some model animals used in biomedical research, as well as endangered animals (Fig 1).

Binding of the spike protein of SARS-CoV-2 with ACE2 is a prerequisite for viral entry. To examine this interaction, we employed a cell-based assay to assess the binding of SARS-CoV-2 spike protein with cell surface-displayed ACE2 protein using flow cytometry. We cloned the cDNA of 49 ACE2 orthologs (mouse ACE2 is included as the negative control) into a bicistronic lentiviral vector (pLVX-IRES-zsGreen1) to express the ACE2 protein with FLAG tag at the C-terminal and expression of a fluorescent protein zsGreen1 driven by IRES element is used to monitor the transduction efficiency. The expression of ACE2 orthologs in HeLa cells were assessed by Western blotting using the FLAG antibody. All the 49 ACE2 proteins were expressed and readily detected at the 100-130 kDa, due to the varying degree of glycosylation (Fig. 2A).

Next, purified S1 domain of SARS-CoV-2 spike protein fused with the Fc proteins (S1-Fc) were incubated with HeLa cells expressing ACE2 orthologs, and the binding of S1-Fc with ACE2 proteins was determined by flow cytometry. The binding efficiency was defined as the percentage of S1 protein positive population in zsGreen1 cells. As expected, the binding of mouse ACE2 with viral spike protein is very low, similar to the empty vector control, whereas, human ACE2 could efficiently bind S1-Fc protein, consistent with previously findings (Wan et al., 2020; Zhou et al., 2020). Surprisingly, we found that, with exception of *Callithrix jacchus* (White-tufted-ear marmoset, #11), *Saimiri boliviensis boliviensis* (Bolivian squirrel monkey, #12), *Sapajus apella* (Tufted capuchin, #13), all belonging to New World monkeys with no detectable binding, *Phascolarctos cinereus* (Koala, #34) and *Mustela ermine* (Stoat, #44), both with limited binding, all other ACE2 proteins from 44 species (44/49 species) could bind well with the S1 of spike protein, albeit with different efficiencies in comparison to that of the human ACE2 (Fig. 2B). The limited or undetectable binding of ACE2 with viral spike proteins is not due to the low expression of ACE2 as indicated by Western blotting assay (Fig 2A). Our findings were consistent with the recent report that SARS-CoV-2 could experimentally establish infection in old world monkeys (*Macaca mulatta* and *Macaca fascicularis*), instead of New World monkeys (*Callithrix jacchus*) (Lu et al., 2020).

In summary, this result suggested that a diversity of ACE2 proteins could interact with SARS-CoV-2 spike protein, implying their high potential to mediate virus entry.

Functional assessment of ACE2 orthologs for SARS-CoV-2 entry

It has been shown that HeLa cells lacking expression of endogenous ACE2 were not permissive

to SARS-CoV-2 infection (Zhou et al., 2020). To directly test the function of ACE2 orthologs mediating viral entry, we performed genetic complementation experiment in HeLa cells to evaluate ACE2 orthologs function to mediate virus entry.

The HeLa cells ectopically expressed individual ACE2 protein were infected with SARS-CoV-2 (moi=1). At 48 h post-infection, the complemented HeLa cells were fixed to perform the immunofluorescent staining of intracellular viral nucleocapsid protein, an indicator of virus replication. As expected, HeLa cells expressing mouse ACE2, were still not permissive to SARS-CoV-2 infection, while human ACE2 rendered them permissiveness. Consistent with the results from ACE2 binding with viral S1 spike protein, HeLa cells expressing ACE2 orthologs from *Callithrix jacchus* (White-tufted-ear marmoset, #11), *Saimiri boliviensis boliviensis* (Bolivian squirrel monkey, #12), *Sapajus apella* (Tufted capuchin, #13), or *Phascolarctos cinereus* (Koala, #34) were non-permissive to SARS-CoV-2 infection; HeLa cells expressing ACE2 from *Mustela erminea* (Stoat, #44) was permissive, albeit with low efficiency; all other 44 ACE2 orthologs among the 49 species could rendered the HeLa cell permissive to SARS-CoV-2 infection, as indicated by the detection of large number of nucleocapsid positive signal in zsGreen1 population (Fig. 3).

Collectively, our results demonstrated that SARS-CoV-2 can utilize ACE2 from evolutionarily diverse species of mammals as the cellular receptor for viral entry, suggesting that SARS-CoV-2 probably has a broad host range.

The potential genetic determinants of ACE2 from New World monkeys to restrict SARS-CoV-2 entry

Although the overall protein sequences of ACE2 are largely conserved across all tested species (71–100% identity compared with human ACE2) (Fig.4A), the conservation of ACE2 does not necessarily correlate with its function to support virus entry. For example, as shown in Fig. 3 and Fig. 4, ACE2 orthologs from New World monkeys *Callithrix jacchus* (White-tufted-ear marmoset, #11), *Sapajus apella* (Tufted capuchin, #12), and *Saimiri boliviensis boliviensis* (Bolivian squirrel monkey, #13) exhibited limited or undetectable receptor activity to mediate SARS-CoV-2 entry, despite that they share 92-93% identity with human ACE2. In contrary, the ACE2 proteins from *Bos Taurus* (cattle, #28) or *Sus scrofa* (pig, #20) could efficiently facilitate virus entry, with 78% or 81% identity with human ACE2, respectively (Fig. 4A). It is conceivable that there are critical residues in ACE2 proteins from New World monkeys as the genetic determinant to restrict viral entry.

New World monkeys are widely used as model animals in the biomedical research. Our results showed that their ACE2 proteins cannot bind SARS-CoV-2 spike protein and promote virus entry, which is in line with a recent finding *in vivo* that *Callithrix jacchus* (White-tufted-ear marmoset) are resistant to virus infection (Lu et al., 2020). To identify the genetic determinant of ACE2 orthologs from New World monkeys for restricting viral entry, we analyzed ACE2 protein contact sites with viral spike protein, especially the amino acid residues that form hydrogen bonds or salt

bridge with viral S protein, such as Q24, D30, E35, E37, D38, Y41, Q42, Y83, K353 and R393 (Lan et al., 2020; Shang et al., 2020; Yan et al., 2020). Through alignment with other ACE2 proteins, that could support SARS-CoV-2 entry, we found that the only sequence difference in ACE2 from New World monkeys is H and E at position 41 and 42, instead of Y41 and Q42, respectively, at the interface of receptor-spike complex (Fig.1). At the human ACE2 41 position, the OH atom of tyrosine forms hydrogen bonds with side chain OG1 atom of T500 and main chain N atom of N501 of the SARS-CoV-2 spike protein. The NE2 atom of 42Q of human ACE2 forms hydrogen bonds with main chain O atom of G446 and side chain OH atom of Y449 of the SARS-CoV-2 spike protein. The mutations at these two consecutive 41 and 42 positions may disrupt the hydrogen-bonding interactions and impair the binding of New World monkeys ACE2 with SARS-CoV-2 spike (Fig. 4B). Thus, our analysis identifies the potential genetic determinant of ACE2 function as the cellular receptor and provides greater insight into the species-specific restriction of SARS-CoV-2 cell entry, which can inform the development of animal models.

Discussion

To prevent the zoonotic transmission of SARS-CoV-2 to human, the identification of animal reservoirs or intermediate hosts of SARS-CoV-2 is of great significance. Recently, a coronavirus closely related to SARS-CoV-2 in pangolins was identified, and this virus showed 90% of sequence identity to that of SARS-CoV-2 (Lam et al., 2020; Zhang et al., 2020b). However, the result of phylogenetic analysis does not support the notion that pangolins is the intermediate host of SARS-CoV-2. The host range and animal reservoirs of SARS-CoV-2 remain to be explored.

For the cross-species transmission of SARS-CoV-2 from the intermediate hosts to humans, the virus needs to overcome at least two main host genetic barriers: the specificity of viral spike-ACE2 receptor interactions and the ability of virus to escape from the host antiviral immunity. Virus-receptor specific interaction is the first step to initiate virus infection and is a critical determinant of host species range and tissue tropism. SARS-CoV-2 uses cellular receptor ACE2 in a species-specific manner. Human, palm civet, bat and pig ACE2 could support the virus entry, however, mouse ACE2 cannot (Zhou et al., 2020). To explore the possible SARS-CoV-2 animal reservoirs and intermediate hosts, we analyzed the ACE2 genes from the vertebrates, particularly from the mammals. Our results suggested that ACE2 orthologs are largely conserved, implying the importance of its physiological functions. Surprisingly, we also found that ACE2 orthologs from a wide range of mammals could act as functional receptor to mediate SARS-CoV-2 infection when ectopically expressed in HeLa cells, suggesting that SARS-CoV-2 may have a diversity of host ranges and intermediate hosts.

It is of note that our findings are based on functional study of ACE2 proteins with authentic virus infection instead of pseudotyped virus. Our results are also confirmed by the recent *in vivo* findings that ferret, cat, dogs, and Old World monkeys are susceptible to SARS-CoV-2 infection but not the marmoset, which is the New World monkey (Lu et al., 2020; Shi et al., 2020; Zhang et al., 2020a). The host range or specificity of a virus is limited by complex reasons. The lack of host dependency factors or the incompatibility of host orthologs restricts the virus infection. Alternatively, the capability to evade the antiviral immune response of a given host can also shape species tropism of viruses (Ding et al., 2018; Douam et al., 2015).

Development of prophylactic vaccines or effective antivirals are urgently needed to combat SARS-CoV-2 infection (Rome and Avorn, 2020). Establishment of ideal animal models to evaluate of the efficacy of vaccine candidates and antiviral strategies against SARS-CoV-2 *in vivo* is of importance. Additionally, there is a need with suitable laboratory animals to understand the viral transmission and pathogenesis. Human ACE2 transgenic mouse has been used for the study of SARS-CoV and SARS-CoV-2 *in vivo* (Bao et al., 2020; Yang et al., 2007). However, the unphysiologically high expression level of ACE2 driven by universal promotor may not recapitulate the human disease caused by SARS-CoV-2. Recently, the ferret has been used to assess the SARS-CoV-2 infection and transmission. Recently, ferret was used as the animal model for detailed

analysis of SARS-CoV-2 infection and transmission (Kim et al., 2020). Our study examined the usage of receptor ACE2 from multiple species of laboratory animals, for example, ferret, crab-eating macaque, Chinese hamster etc. It is plausible to test other species that the ACE2 could serve as functional entry receptor as animal models to facilitate the evaluation of SARS-CoV-2 therapeutics and vaccines.

ACE2 orthologs from *Sapajus apella*, *Saimiri boliviensis boliviensis* and *Callithrix jacchus*, all belonging to New World monkeys, cannot support SARS-CoV-2 entry. The species-specific residues H41 and E42 of ACE2 were identified in these species as the possible genetic restriction polymorphisms. It is worthwhile to determine whether the swapping of these critical amino acids with human residues could rescue the entry of SARS-CoV-2.

Our unexpected finding that SARS-CoV-2 uses ACE2 from diverse species warns the importance of surveillance of animals in close contact with humans. We found that pet animals such as cat and dog, livestock animals such as pigs, cattle, rabbits, sheep, horses, and goats, and even some animals in the zoo or aquarium may serve as the intermediate hosts for virus transmission. Our study also identified the broad range of wild animals as the potential susceptible hosts of SARS-CoV-2, highlighting the importance of banning illegal wildlife trade and consumption.

In all, this is the first study to functionally assess the ACE2 orthologs from nearly 50 mammalian hosts using the authentic SARS-CoV-2 virus, which provides new insight into the potential host range and cross-species transmission. It also suggests that SARS-CoV-2 might be distributed much more widely than previously recognized, emphasizing the necessity to monitor the susceptible hosts, especially their potential of causing zoonosis, which could prevent the future outbreaks.

ACKNOWLEDGEMENT

We thank Professor Jin Zhong (Institut Pasteur of Shanghai, CAS) for revision of the manuscript. We wish to acknowledge Di Qu, Zhiping Sun, Wendong Han and the others at Biosafety Level 3 Laboratory of Fudan University for experiment design and technical assistance. We are grateful to Yingjie Zhang and Ruiqi Chen (Tsinghua University) for confirmation of the gene sequences information.

This work was supported by Tsinghua-Peking University Center of Life Sciences (045-61020100120), National Natural Science Foundation of China (32041005), Tsinghua University Initiative Scientific Research Program (2019Z06QCX10), Beijing Advanced Innovation Center for Structure Biology (100300001), Start-up Foundation of Tsinghua University (53332101319), Shanghai Municipal Science and Technology Major Project (20431900400) and Project of Novel Coronavirus Research of Fudan University.

MATERIALS AND METHODS

Cell cultures and SARS-CoV-2 virus. HEK293T cells (American Tissue Culture Collection, ATCC, Manassas, VA, CRL-3216), Vero E6 (Cell Bank of the Chinese Academy of Sciences, Shanghai, China) and HeLa (ATCC #CCL-2) were maintained in Dulbecco's modified Eagle medium (DMEM) (Gibco, NY, USA) supplemented with 10% (vol/vol) fetal bovine serum (FBS), 10mM HEPES, 1mM sodium pyruvate, 1×non-essential amino acids, and 50 IU/ml penicillin/streptomycin in a humidified 5% (vol/vol) CO₂ incubator at 37°C. Cells were tested routinely and found to be free of mycoplasma contamination. The SARS-CoV-2 strain nCoV-SH01 (GenBank accession no. MT121215) was isolated from a COVID-19 patient and propagated in Vero E6 cells for use. All experiments involving virus infections were performed in the biosafety level 3 facility of Fudan University following the regulations.

Plasmids. The cDNAs encoding ACE2 orthologs (Table S1) were synthesized by GenScript and cloned into pLVX-IRES-zsGreen1 vectors (Catalog No. 632187, Clontech Laboratories, Inc) with an C-terminal FLAG tag. All the plasmids were verified by Sanger sequencing.

Lentivirus production. Vesicular stomatitis virus G protein (VSV-G) pseudotyped lentiviruses expressing ACE2 orthologs tagged with FLAG at the C-terminus were produced by transient co-transfection of the third-generation packaging plasmids pMD2G (Addgene #12259) and psPAX2 (Addgene #12260) and the transfer vector with VigoFect DNA transfection reagent (Vigorous) into HEK293T cells. The medium was changed 12 h post transfection. Supernatants were collected at 24 and 48h after transfection, pooled, passed through a 0.45- μ m filter, aliquoted, and frozen at -80°C.

Phylogenetic analysis and sequence alignment. The amino acid sequences of ACE2 orthologs for jawed vertebrates (Gnathostomata) were exported from the NCBI nucleotide database. Numbers in each sequence correspond to the GenBank accession number. 81 sequences were collected for the presence of five critical viral spike-contacting residues of ACE2 corresponding to amino acids Lys31, Glu35, Asp38, Met82 and Lys353 in human ACE2 (NM_001371415.1). The protein sequences of different species were then passed into MEGA-X (Version 10.05) software for further analysis. The alignment was conducted using the MUSCLE algorithm. Then the alignment file was used to construct the phylogenetic tree. We used the Neighbor Joining option of the MEGA-X and the default parameters to build the tree.

Western blotting assay. Sodium dodecyl sulfate-polyacrylamide gel electrophoresis (SDS-PAGE) immunoblotting was performed as follows: After trypsinization and cell pelleting at 2,000 × g for 10 min, whole-cell lysates were harvested in RIPA lysis buffer (50 mM Tris-HCl [pH 8.0], 150mM NaCl, 1% NP-40, 0.5% sodium deoxycholate, and 0.1% SDS) supplemented with protease inhibitor cocktail (Sigma). Lysates were electrophoresed in 12% polyacrylamide gels and transferred onto nitrocellulose membrane. The blots were blocked at room temperature for 0.5 h using 5% nonfat milk in 1× phosphate-buffered saline (PBS) containing 0.1% (v/v) Tween 20. The blots were

exposed to primary antibodies anti- β -Tubulin (CW0098, CWBIO), or anti-FLAG (F7425, Sigma) in 5% nonfat milk in 1 \times PBS containing 0.1% Tween 20 for 2 h. The blots were then washed in 1 \times PBS containing 0.1% Tween 20. After 1h exposure to HRP-conjugated secondary antibodies, subsequent washes were performed and membranes were visualized using the Luminescent image analyzer (GE).

Surface ACE2 binding assay. HeLa cells were transduced with lentiviruses expressing the ACE2 from different species for 48 h. The cells were collected with TrypLE (Thermo #12605010) and washed twice with cold PBS. Live cells were incubated with the recombinant protein, S1 domain of SARS-CoV-2 spike C-terminally fused with Fc (Sino Biological #40591-V02H, 1 μ g/ml) at 4 °C for 30 min. After washing, cells were stained with goat anti-human IgG (H + L) conjugated with Alexa Fluor 647 (Thermo #A21445, 2 μ g/ml) for 30 min at 4 °C. Cells were then washed twice and subjected to flow cytometry analysis (Thermo, Attune™ NxT).

Immunofluorescence staining of viral nucleocapsid. HeLa cells were transduced with lentiviruses expressing the ACE2 from different species for 48 h. Cells were then infected with nCoV-SH01 at an MOI of 1 for 1 h, washed three times with PBS, and incubated in 2% FBS culture medium for 48 h for viral antigen staining. Cells were fixed with 4% paraformaldehyde in PBS, permeabilized with 0.2% Triton X-100, and incubated with the rabbit polyclonal antibody against SARS-CoV nucleocapsid protein (Rockland, 200-401-A50, 1 μ g/ml) at 4 °C overnight. After three times of washing, cells were incubated with the secondary goat anti-rabbit antibody conjugated with Alexa Fluor 488 (Thermo #A11034, 2 μ g/ml) for 2 h at room temperature, followed by staining with 4',6-diamidino-2-phenylindole (DAPI). Images were collected using an EVOS™ Microscope M5000 Imaging System (Thermo #AMF5000). Images were processed using the ImageJ program (<http://rsb.info.nih.gov/ij/>).

Statistics analysis. One-way analysis of variance (ANOVA) with Tukey's honestly significant difference (HSD) test was used to test for statistical significance of the differences between the different group parameters. *P* values of less than 0.05 were considered statistically significant.

FIGURE LEGENDS

Figure 1. Phylogenetic analysis of ACE2 orthologs with potential to support the SARS-CoV-2 entry and alignment of amino acids of ACE2 at the interaction interface with viral spike protein. The ACE2 protein sequences (Supplemental Table 1), as well as *Mus musculus* (mouse) and *Rattus norvegicus* (rat) ACE2, were chosen and analyzed by MEGA-X (Version 10.05) software and MUSCLE algorithm. The phylogenetic tree was built using Neighbor Joining method of the MEGA-X. The contacting residues of human ACE2 (a distance cutoff 4 Å) at the SARS-CoV-2 RBD/ACE2 interfaces are shown, and the contacting network involves at least 20 residues in ACE2 and 10 residues in the SARS-CoV-2 RBD, which are listed and connected with solid line. Black lines indicate hydrogen bonds, and red line represents salt-bridge interaction. The tested species are highlighted as purple and the ID number of each species in the following experiment is labeled on the right. Only the amino acids different from human are shown.

Figure 2. Binding of ACE2 orthologs with SARS-CoV-2 spike protein. (A) HeLa cells transduced with lentiviruses expressing FLAG-tagged ACE2 orthologs were subjected to immunoblotting assay. Tubulin was served as the loading control. (B) HeLa cells were transduced with ACE2 orthologs of the indicated species, and the surface displayed ACE2 proteins were detected by incubating with the recombinant S1 domain of SARS-CoV-2 spike C-terminally fused with Fc, followed by staining with goat anti-human IgG (H + L) conjugated with Alexa Fluor 647 for flow cytometry analysis.

Figure 3. Functional assessment of ACE2 orthologs mediating SARS-CoV-2 virus entry. HeLa cells transduced with lentiviruses expressing ACE2 orthologs or empty vector were infected with SARS-CoV-2 virus (MOI=1). Immunofluorescence assay was performed to detect the expression of viral nucleocapsid protein. Viral nucleocapsid (N) protein (red) and nuclei (blue) was shown. Green signal indicated the transduction efficiency of ACE2 orthologs. *Callithrix jacchus* (White-tufted-ear marmoset, #11), *Saimiri boliviensis boliviensis* (Bolivian squirrel monkey, #12), *Sapajus apella* (Tufted capuchin, #13), and *Phascolarctos cinereus* (Koala, #34) were non-permissive to SARS-CoV-2 infection, highlighted as purple. The images were merged and edited by Image J software.

Figure 4. Identification of the species-specific genetic determinant of ACE2 restriction of SARS-CoV-2 entry. (A) Protein sequence identity matrices of ACE2 from the tested species. The ACE2 sequences from different species were analyzed using SIAS (Sequence Identity And Similarity) tool (<http://imed.med.ucm.es/Tools/sias.html>) to determine the identity of ACE2 proteins across different species. (B) The binding interface of human ACE2 with SARS-CoV-2 RBD surrounding the ACE2 Y41 and Q42. Residue Y41 forms hydrogen bonds with T500 and N501 of

SARS-CoV-2 RBD, and Q42 could also interact with G446 or Y449 by hydrogen bonds. The mutations in the New World monkeys ACE2, especially the Y41H replacement may disrupt the hydrogen-bonding interactions and impair the binding with SARS-CoV-2 spike. The PDB code of the complex of human ACE2 with SARS-CoV-2: 6M0J.

SUPPLEMENTAL INFORMATION

Supplemental Figure 1. ACE2 orthologs selection from the jawed vertebrates. ACE2 orthologs were recorded in the NCBI dataset and further parsed to 80 ACE2 orthologs with potential function of supporting SARS-CoV-2 entry, based on the conserved property of 5 amino acids required for the binding between receptor ACE2 and SARS-CoV spike protein (Li, 2008, 2015; Li et al., 2005; Wan et al., 2020).

FIGURES

Figure 1

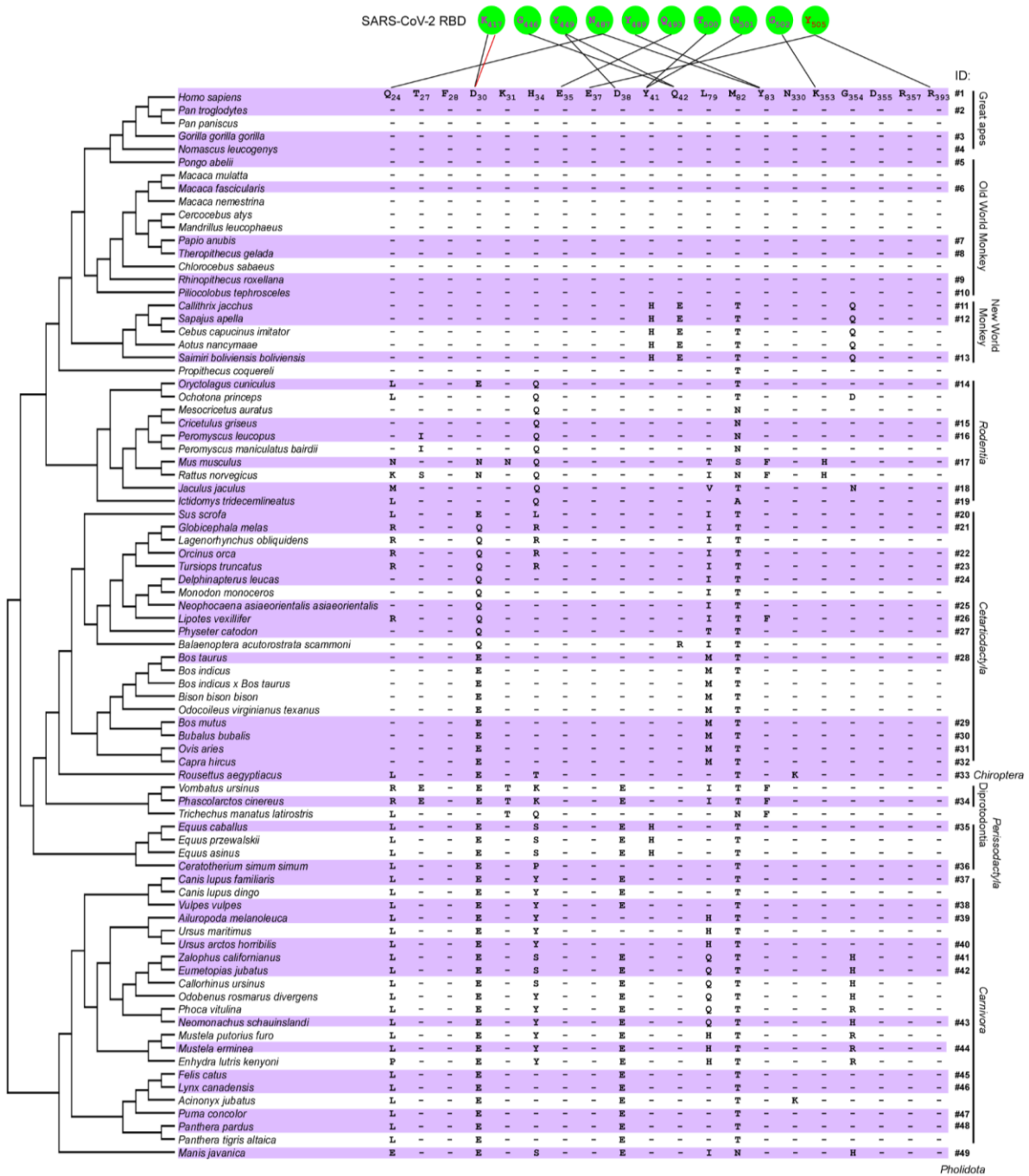


Figure 2

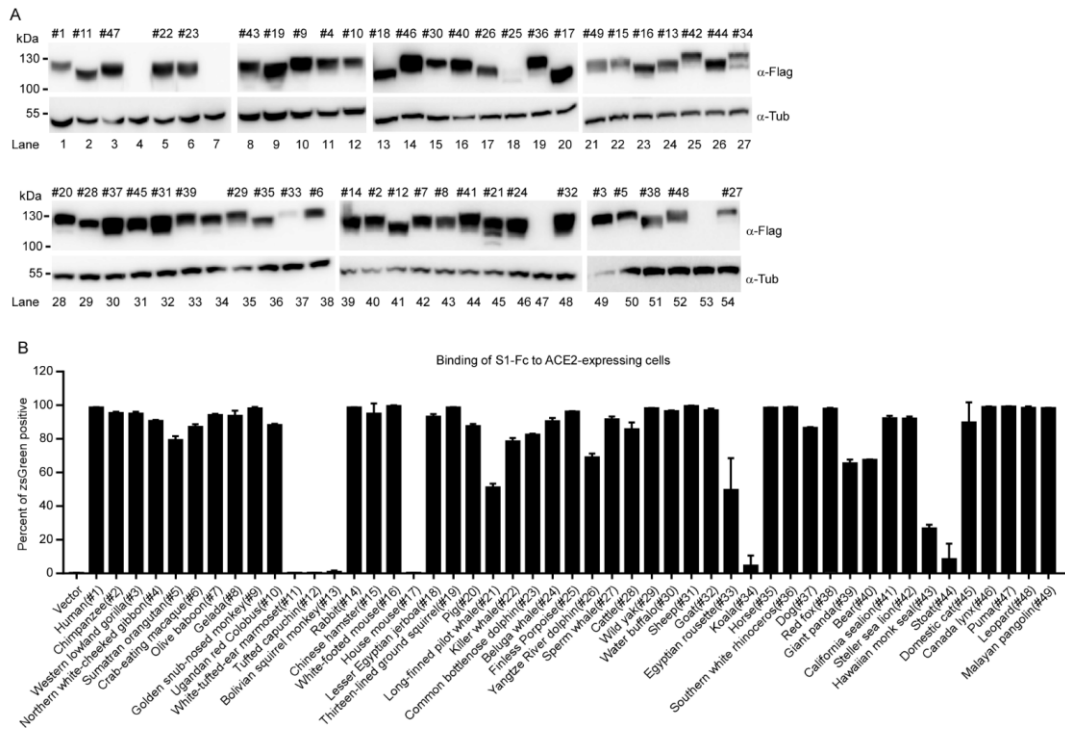
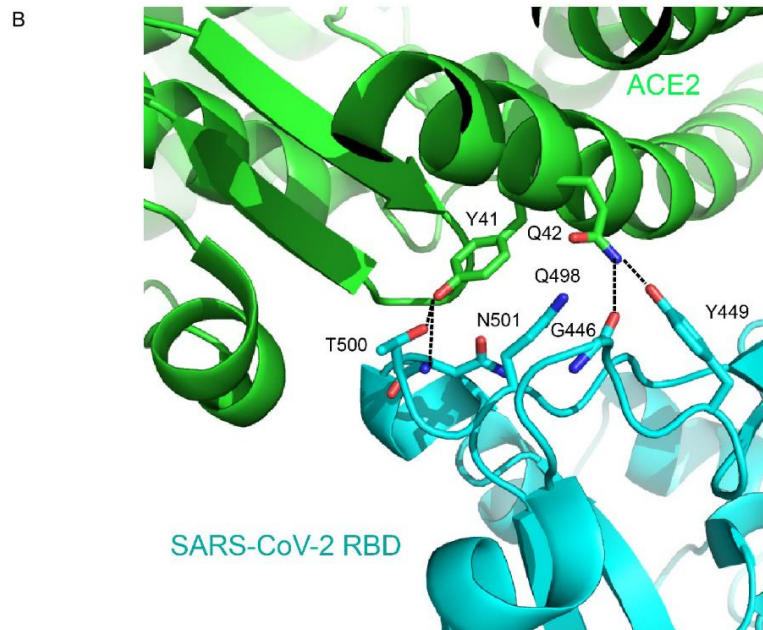
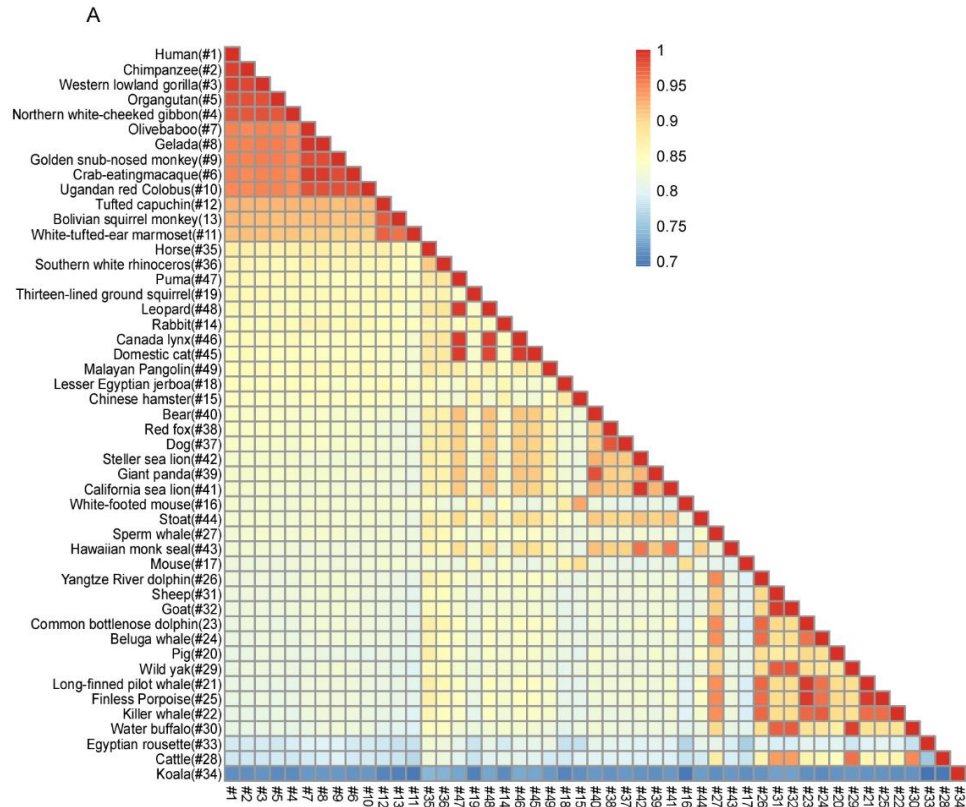


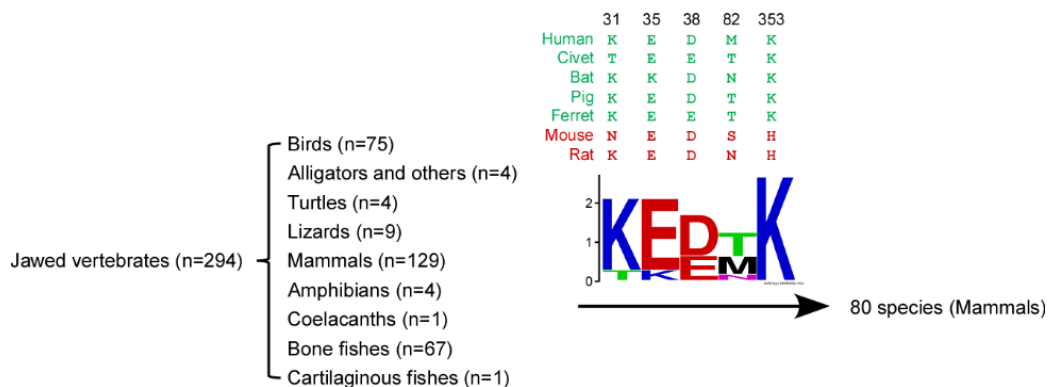
Figure 3



Figure 4



Supplemental Figure 1



Supplemental Table 1: ACE proteins with potential susceptibility to SARS-CoV-2 entry

| ID | Species | Common Name | NCBI Accession # |
|-----|--|--------------------------------|------------------|
| #1 | <i>Homo sapiens</i> | Human | NP_001358344.1 |
| #2 | <i>Pan troglodytes</i> | Chimpanzee | XP_016798468.1 |
| #3 | <i>Gorilla gorilla gorilla</i> | Western lowland gorilla | XP_018874749.1 |
| #4 | <i>Nomascus leucogenys</i> | Northern white-cheeked gibbon | XP_003261132.2 |
| #5 | <i>Pongo abeli</i> | Sumatran orangutan | NP_001124604.1 |
| #6 | <i>Macaca fascicularis</i> | Crab-eating macaque | XP_005593094.1 |
| #7 | <i>Papio anubis</i> | Olive baboon | XP_021788732.1 |
| #8 | <i>Theropithecus gelada</i> | Gelada | XP_025227847.1 |
| #9 | <i>Rhinopithecus roxellana</i> | Golden snub-nosed monkey | XP_010364367.2 |
| #10 | <i>Ptilocolobus tephrosceles</i> | Ugandan red Colobus | XP_023054821.1 |
| #11 | <i>Callithrix jacchus</i> | White-tufted-ear marmoset | XP_008987241.1 |
| #12 | <i>Sapajus apella</i> | Tufted capuchin | XP_032141854.1 |
| #13 | <i>Saimiri boliviensis boliviensis</i> | Bolivian squirrel monkey | XP_010334925.1 |
| #14 | <i>Oryctolagus cuniculus</i> | Rabbit | XP_002719891.1 |
| #15 | <i>Cricetulus griseus</i> | Chinese hamster | XP_003503283.1 |
| #16 | <i>Peromyscus leucopus</i> | White-footed mouse | XP_028743609.1 |
| #17 | <i>Mus musculus</i> | House mouse | NP_001123985.1 |
| #18 | <i>Jaculus jaculus</i> | Lesser Egyptian jerboa | XP_004671523.1 |
| #19 | <i>Ictidomys tridecemlineatus</i> | Thirteen-lined ground squirrel | XP_005316051.3 |
| #20 | <i>Sus scrofa</i> | Pig | NP_001116542.1 |
| #21 | <i>Globicephala melas</i> | Long-finned pilot whale | XP_030703991.1 |
| #22 | <i>Orcinus orca</i> | Killer whale | XP_004269705.1 |
| #23 | <i>Tursiops truncatus</i> | Common bottlenose dolphin | XP_019781177.1 |
| #24 | <i>Delphinapterus leucas</i> | Beluga whale | XP_022418360.1 |
| #25 | <i>Neophocaena asiaeorientalis asiaeorientalis</i> | Finless Propoise | XP_024599894.1 |
| #26 | <i>Lipotes vexillifer</i> | Yangtze River dolphin | XP_007466389.1 |
| #27 | <i>Physeter catodon</i> | Sperm whale | XP_023971279.1 |
| #28 | <i>Bos taurus</i> | Cattle | XP_005228485.1 |
| #29 | <i>Bos mutus</i> | Wild yak | XP_005903173.1 |
| #30 | <i>Bubalus bubalis</i> | Water buffalo | XP_006041602.1 |
| #31 | <i>Ovis aries</i> | Sheep | XP_011961657.1 |
| #32 | <i>Capra hircus</i> | Goat | NP_001277036.1 |
| #33 | <i>Rousettus aegyptiacus</i> | Egyptian rousette | XP_015974412.1 |
| #34 | <i>Phascolarctos cinereus</i> | Koala | XP_020863153.1 |
| #35 | <i>Equus caballus</i> | Horse | XP_001490241.1 |
| #36 | <i>Ceratotherium simum simum</i> | Southern white rhinoceros | XP_004435206.1 |
| #37 | <i>Canis lupus familiaris</i> | Dog | NP_001158732.1 |
| #38 | <i>Vulpes vulpes</i> | Red fox | XP_025842512.1 |
| #39 | <i>Ailuropoda melanoleuca</i> | Giant panda | XP_002930657.1 |
| #40 | <i>Ursus arctos horribilis</i> | Bear | XP_026333865.1 |
| #41 | <i>Zalophus californianus</i> | California sea lion | XP_027465353.1 |
| #42 | <i>Eumetopias jubatus</i> | Steller sea lion | XP_027970822.1 |
| #43 | <i>Neomonachus schauinslandi</i> | Hawaiian monk seal | XP_021536480.1 |
| #44 | <i>Mustela erminea</i> | Stoat | XP_032187677.1 |
| #45 | <i>Felis catus</i> | Domestic cat | XP_023104564.1 |
| #46 | <i>Lynx canadensis</i> | Canada lynx | XP_030160839.1 |
| #47 | <i>Puma concolor</i> | Puma | XP_025790417.1 |
| #48 | <i>Panthera pardus</i> | Leopard | XP_019273508.1 |
| #49 | <i>Manis javanica</i> | Malayan pangolin | XP_017505746.1 |

Supplemental Table 2: ACE2 proteins predicted unsusceptible to SARS-CoV-2 entry

| Species | Common Name | NCBI Accession # |
|---------------------------------|--|------------------|
| <i>Mus musculus</i> | House mouse | NP_001123985.1 |
| <i>Rattus norvegicus</i> | Norway rat | NP_001012006.1 |
| <i>Myotis brandtii</i> | Brandts bat | XP_014399780.1 |
| <i>Heterocephalus glaber</i> | Naked mole-rat | XP_004866157.1 |
| <i>Monodelphis domestica</i> | Gray short-tailed opossum | XP_007500935.1 |
| <i>Sarcophilus harrisii</i> | Tasmanian devil | XP_031814825.1 |
| <i>Dipodomys ordii</i> | Ords kangaroo rat | XP_012887572.1 |
| <i>Mus caroli</i> | Ryukyu mouse | XP_021009138.1 |
| <i>Mus pahari</i> | Shrew mouse | XP_021043935.1 |
| <i>Grammomys surdaster</i> | Grammomys surdaster | XP_028617961.1 |
| <i>Mastomys coucha</i> | Southern multimammate mouse | XP_031226742.1 |
| <i>Nannospalax galili</i> | Upper Galilee mountains blind mole rat | XP_008839098.1 |
| <i>Microtus ochrogaster</i> | Prairie vole | XP_005358818.1 |
| <i>Cavia porcellus</i> | Domestic guinea pig | XP_023417808.1 |
| <i>Chinchilla lanigera</i> | Long-tailed chinchilla | XP_013362428.1 |
| <i>Octodon degus</i> | Degu | XP_023575315.1 |
| <i>Fukomys damarensis</i> | Damara mole-rat | XP_010643477.1 |
| <i>Marmota marmota marmota</i> | Alpine marmot | XP_015343540.1 |
| <i>Urocyon parryi</i> | Arctic ground squirrel | XP_026252505.1 |
| <i>Marmota flaviventris</i> | Yellow-bellied marmot | XP_027802308.1 |
| <i>Suricata suricatta</i> | meerkat | XP_029786256.1 |
| <i>Vicugna pacos</i> | Alpaca | XP_006212709.1 |
| <i>Camelus ferus</i> | Wild Bactrian camel | XP_006194263.1 |
| <i>Camelus bactrianus</i> | Bactrian camel | XP_010966303.1 |
| <i>Camelus dromedarius</i> | Arabian camel | XP_010991717.1 |
| <i>Erinaceus europaeus</i> | Western European hedgehog | XP_007538670.1 |
| <i>Sorex araneus</i> | European shrew | XP_004612266.1 |
| <i>Condylura cristata</i> | Star-nosed mole | XP_012585871.1 |
| <i>Pteropus vampyrus</i> | Large flying fox | XP_011361275.1 |
| <i>Pteropus alecto</i> | Black flying fox | XP_006911709.1 |
| <i>Desmodus rotundus</i> | Common vampire bat | XP_024425698.1 |
| <i>Phyllostomus discolor</i> | Pale spear-nosed bat | XP_028378317.1 |
| <i>Miniopterus natalensis</i> | Natal long-fingered bat | XP_016058453.1 |
| <i>Hipposideros armiger</i> | Great roundleaf bat | XP_019522936.1 |
| <i>Eptesicus fuscus</i> | Big brown bat | XP_008153150.1 |
| <i>Myotis davidii</i> | David's myotis | XP_006775273.1 |
| <i>Myotis lucifugus</i> | Little brown bat | XP_023609437.1 |
| <i>Tupaia chinensis</i> | Chinese tree shrew | XP_006164754.1 |
| <i>Rhinopithecus bieti</i> | Black snub-nosed monkey | XP_017744069.1 |
| <i>Carlito syrichta</i> | Philippine tarsier | XP_008062810.1 |
| <i>Microcebus murinus</i> | Gray mouse lemur | XP_020140826.1 |
| <i>Otolemur garnettii</i> | Small-eared galago | XP_003791912.1 |
| <i>Orycteropus afer afer</i> | Aardvark | XP_007951028.1 |
| <i>Elephantulus edwardii</i> | Cape elephant shrew | XP_006892457.1 |
| <i>Echinops telfairi</i> | Small Madagascar hedgehog | XP_004710002.1 |
| <i>Chrysochloris asiatica</i> | Cape golden mole | XP_006835673.1 |
| <i>Loxodonta africana</i> | African savanna elephant | XP_023410960.1 |
| <i>Dasyurus novemcinctus</i> | Nine-banded armadillo | XP_004449124.1 |
| <i>Ornithorhynchus anatinus</i> | Platypus | XP_001515597.2 |

References

- Bao, L., Deng, W., Huang, B., Gao, H., Liu, J., Ren, L., Wei, Q., Yu, P., Xu, Y., Qi, F., *et al.* (2020). The Pathogenicity of SARS-CoV-2 in hACE2 Transgenic Mice. *bioRxiv*.
- Cui, J., Li, F., and Shi, Z.L. (2019). Origin and evolution of pathogenic coronaviruses. *Nat Rev Microbiol* *17*, 181-192.
- Ding, Q., Gaska, J.M., Douam, F., Wei, L., Kim, D., Balev, M., Heller, B., and Ploss, A. (2018). Species-specific disruption of STING-dependent antiviral cellular defenses by the Zika virus NS2B3 protease. *Proc Natl Acad Sci U S A* *115*, E6310-E6318.
- Douam, F., Gaska, J.M., Winer, B.Y., Ding, Q., von Schaewen, M., and Ploss, A. (2015). Genetic Dissection of the Host Tropism of Human-Tropic Pathogens. *Annu Rev Genet* *49*, 21-45.
- Graham, R.L., Donaldson, E.F., and Baric, R.S. (2013). A decade after SARS: strategies for controlling emerging coronaviruses. *Nat Rev Microbiol* *11*, 836-848.
- Hoffmann, M., Kleine-Weber, H., Schroeder, S., Kruger, N., Herrler, T., Erichsen, S., Schiergens, T.S., Herrler, G., Wu, N.H., Nitsche, A., *et al.* (2020). SARS-CoV-2 Cell Entry Depends on ACE2 and TMPRSS2 and Is Blocked by a Clinically Proven Protease Inhibitor. *Cell*.
- Kim, Y.I., Kim, S.G., Kim, S.M., Kim, E.H., Park, S.J., Yu, K.M., Chang, J.H., Kim, E.J., Lee, S., Casel, M.A.B., *et al.* (2020). Infection and Rapid Transmission of SARS-CoV-2 in Ferrets. *Cell Host Microbe*.
- Lam, T.T., Shum, M.H., Zhu, H.C., Tong, Y.G., Ni, X.B., Liao, Y.S., Wei, W., Cheung, W.Y., Li, W.J., Li, L.F., *et al.* (2020). Identifying SARS-CoV-2 related coronaviruses in Malayan pangolins. *Nature*.
- Lan, J., Ge, J., Yu, J., Shan, S., Zhou, H., Fan, S., Zhang, Q., Shi, X., Wang, Q., Zhang, L., *et al.* (2020). Structure of the SARS-CoV-2 spike receptor-binding domain bound to the ACE2 receptor. *Nature*.
- Li, F. (2008). Structural analysis of major species barriers between humans and palm civets for severe acute respiratory syndrome coronavirus infections. *J Virol* *82*, 6984-6991.
- Li, F. (2015). Receptor recognition mechanisms of coronaviruses: a decade of structural studies. *J Virol* *89*, 1954-1964.
- Li, F., Li, W., Farzan, M., and Harrison, S.C. (2005). Structure of SARS coronavirus spike receptor-binding domain complexed with receptor. *Science* *309*, 1864-1868.
- Lu, S., Zhao, Y., Yu, W., Yang, Y., Gao, J., Wang, J., Kuang, D., Yang, M., Yang, J., Ma, C., *et al.* (2020). Comparison of SARS-CoV-2 infections among 3 species of non-human primates. *bioRxiv*.
- Perlman, S., and Netland, J. (2009). Coronaviruses post-SARS: update on replication and pathogenesis. *Nat Rev Microbiol* *7*, 439-450.
- Rockx, B., Kuiken, T., Herfst, S., Bestebroer, T., Lamers, M.M., Oude Munnink, B.B., de Meulder, D., van Amerongen, G., van den Brand, J., Okba, N.M.A., *et al.* (2020). Comparative pathogenesis of COVID-19, MERS, and SARS in a nonhuman primate model. *Science*.
- Rome, B.N., and Avorn, J. (2020). Drug Evaluation during the Covid-19 Pandemic. *N Engl J Med*.
- Shang, J., Ye, G., Shi, K., Wan, Y., Luo, C., Aihara, H., Geng, Q., Auerbach, A., and Li, F. (2020). Structural basis of receptor recognition by SARS-CoV-2. *Nature*.
- Shi, J., Wen, Z., Zhong, G., Yang, H., Wang, C., Huang, B., Liu, R., He, X., Shuai, L., Sun, Z., *et al.* (2020). Susceptibility of ferrets, cats, dogs, and other domesticated animals to SARS-coronavirus 2. *Science*.
- Wan, Y., Shang, J., Graham, R., Baric, R.S., and Li, F. (2020). Receptor Recognition by the Novel Coronavirus from Wuhan: an Analysis Based on Decade-Long Structural Studies of SARS Coronavirus. *J Virol* *94*.
- Wu, F., Zhao, S., Yu, B., Chen, Y.M., Wang, W., Song, Z.G., Hu, Y., Tao, Z.W., Tian, J.H., Pei, Y.Y., *et*

al. (2020). A new coronavirus associated with human respiratory disease in China. *Nature* *579*, 265-269.

Yan, R., Zhang, Y., Li, Y., Xia, L., Guo, Y., and Zhou, Q. (2020). Structural basis for the recognition of SARS-CoV-2 by full-length human ACE2. *Science* *367*, 1444-1448.

Yang, X.H., Deng, W., Tong, Z., Liu, Y.X., Zhang, L.F., Zhu, H., Gao, H., Huang, L., Liu, Y.L., Ma, C.M., *et al.* (2007). Mice transgenic for human angiotensin-converting enzyme 2 provide a model for SARS coronavirus infection. *Comp Med* *57*, 450-459.

Zhang, Q., Zhang, H., Huang, K., Yang, Y., Hui, X., Gao, J., He, X., Li, C., Gong, W., Zhang, Y., *et al.* (2020a). SARS-CoV-2 neutralizing serum antibodies in cats: a serological investigation. *bioRxiv*.

Zhang, T., Wu, Q., and Zhang, Z. (2020b). Probable Pangolin Origin of SARS-CoV-2 Associated with the COVID-19 Outbreak. *Curr Biol* *30*, 1346-1351 e1342.

Zhou, P., Yang, X.L., Wang, X.G., Hu, B., Zhang, L., Zhang, W., Si, H.R., Zhu, Y., Li, B., Huang, C.L., *et al.* (2020). A pneumonia outbreak associated with a new coronavirus of probable bat origin. *Nature* *579*, 270-273.